Sixth International Symposium on Turbulence and Shear Flow Phenomena
Seoul, Korea, 22-24 June 2009

FURTHER STUDIES ON THE STATISTICS AND STRUCTURES OF FLAT-PLATE BOUNDARY LAYER WITH PASSING WAKES

Jean-Pierre Hickey, Scott Blakie, Calley Gray & Xiaohua Wu
Department of Mechanical Engineering,
Royal Military College of Canada
PO Box 17 000, Station Forces, K7K 7B4
Kingston, Ontario, Canada
jean-pierre.hickey@rmc.ca

ABSTRACT

Two flat-plate boundary layers with free-stream periodically passing planar wakes in the absence of external pressure gradients were simulated from momentum thickness Reynolds number $Re_\theta = 80$ to fully turbulent for the purpose of addressing several statistical and structural questions identified from recent studies. In the constrained simulation design, the wakes are restricted to six boundary layer thicknesses away from the wall at the inlet, while in the other design the wakes are unconstrained with respect to the boundary layer. The boundary layer statistics before, during and after transition are thoroughly evaluated through comparison with theoretical and experimental data of the zero pressure gradient flat-plate boundary layer. Systematic three-dimensional flow visualizations definitively reveal the precise instant and location of breakdown events, the breakdown mechanism as well as the development after breakdown. Breakdown in both designs is always preceded by the occurrence of braid-like Kelvin-Helmholtz wave packets of small wavelength superimposed on the flank of selected backward streaky structures near the boundary layer outer edge. The small wavelength braids are subsequently replaced by large wavelength Kelvin-Helmholtz structures oriented obliquely with reference to the main body of the streaks, which directly lead to breakdown, see figure 1. Matured turbulent spots have arrowheads directing upstream. But, if a spot originates from the simultaneous breakdown of multiple nearby streaks its arrowhead configuration will be less sharp. Streaks in the present boundary layers are not of rectangular box shape, rather, they are of wedged shape with diminishing strength towards the wall and towards the upstream direction. Despite this and despite the intermittency of the periodically passing wake disturbances, statistics in the early transitional region exhibit characteristics in agreement with previous studies on boundary layer under the continuous perturbation of free-stream isotropic turbulence. It is further found that statistically the present turbulent boundary layers differ from the canonical boundary layer only mildly near the outer edge. The planar wake introduced in the free-stream at $Re_\theta = 80$ is available in raw form so that the inflow condition is precisely defined and repeatable without ambiguity.

INTRODUCTION

We consider an initially laminar incompressible flat-plate boundary layer under the perturbation of free-stream migrating planar wakes at a passing frequency $\mathcal{T}$ but without any imposed streamwise pressure gradient. This setting abstracts from the problem of turbomachinery blade row interaction in that complications arising from geometrical

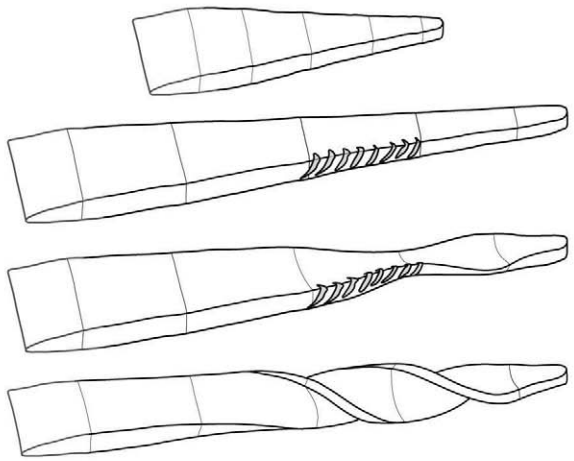

Figure 1: Breakdown mechanism discovered from this study. Top figure: early negative streak; upper-middle: developed negative streak with wrinkle-like small wavelength Kelvin-Helmholtz structure on the flank; lower-middle figure and bottom figure: twisting of negative streak due to large wavelength Kelvin-Helmholtz oscillation.

complexity and pressure gradients are removed. This subject also bears some resemblance to the canonical incompressible zero pressure gradient flat-plate boundary layer (ZPGFPBL) under the perturbation of continuous free-stream isotropic turbulence, although the degree of similarity remains to be quantified.

The rational for this study stems from an initial numerical investigation done by Wu *et al.* (1999) on passing wake induced boundary layer transition. The original simulation of Wu *et al.* (1999) was designed by following the general idea of the earlier experiments of Liu & Rodi (1991) conducted at the university of Karlsruhe. Their experimental results are also broadly consistent with the recent turbomachinery flow experiments performed at Cambridge university, see Stieger (2002), Stieger & Hodson (2004), Hodson & Howell (2005). Although, it should be noted that these Whittle laboratory experiments focused on the interaction between passing wakes and laminar separation bubble. Since the original work by Wu *et al.* , many high quality simulations have been conducted to investigate flat-plate boundary-layer transition. Jacob & Durbin (2001) presented numerical simulation results on flat-plate boundary-layer transition under continuous isotropic free-stream turbulence. They found that the transition precursors consist of long backward jets, which may interact with the free-stream eddies and form turbulent spots in the upper-portion of the boundary layer. In another simulation, Brandt, Schlat-

ter & Henningson (2004) simulated a flat-plate boundary layer transition subjected to controlled free-stream turbulence perturbations. They showed that the small scales can penetrate into the boundary layer and the spanwise scale of the streaks is only weakly dependent on the scales of the free-stream turbulence. Through their investigation, they suggested that the breakdown is related to local instabilities driven by strong shear layers associated with the streaks, the sinuous-like breakdown being driven by the spanwise shear and the varicose-like breakdown by the wall-normal shear. In the last 10 years, many experimental and computational studies on this topic have been undertaken and the purpose of the present work is to address several statistical and structural questions identified from these recent studies.

DETAILS OF PRESENT COMPUTATION

Both constrained and unconstrained cases were simulated with a migrating planar wake with a passing frequency of $\mathcal{T}$ with a mean wake deficit of 14% of the free-stream velocity and a half width of 10% of the unit length. The passing period of the wake, $\mathcal{T}$, is set at 1.67 and the computational domain is defined as $0.1 \leq x/L \leq 3.5$, $0 \leq y/L \leq 0.8$ and $0 \leq z/L \leq 0.2$, where L is the unit length scale. The inlet momentum thickness Reynolds number is $Re_\theta = 80$ and the Reynolds number based on the free-stream velocity U_∞ and L is $Re = 1.5 \times 10^5$. The finite-difference grid size is $2048 \times 400 \times 128$ along the x, y and z directions, respectively. The number of grid points along the streamwise direction used in the present computation is twice of that used in Wu *et al.* (1999). The simulation was performed using 1024 processors on 128 IBM 8-way P655+ nodes. For the constrained wake simulation, the computational time step was fixed at $\delta t = \mathcal{T}/2000 = 0.000835$. For the unconstrained wake simulation, the computational time step was fixed at $\delta t = \mathcal{T}/1000 = 0.00167$. In both case, the initial velocity fields were prescribed as the Blasius profile. The flows were allowed to evolve from the initial unrealistic velocity profile for 20 passing periods $\mathcal{T}$ to reach statistically steady state. Statistics were then collected for another $20\mathcal{T}$. In addition to averaging in time, the statistical sample was enhanced by averaging in the homogeneous spanwise direction. Velocity signals were saved at each time step for a duration of $20\mathcal{T}$ at an array of selected locations for the purpose of frequency spectrum computations.

STATISTICS IN THE TRANSITIONAL REGION

The analysis of the statistical results show that, in the constrained wake setup, there is a very mild pressure gradient in the streamwise direction and that over a large portion of the computational domain it can be considered as nominally zero. The pressure gradient near the inlet of the boundary layer with unconstrained passing wakes is slightly larger due to the impingement of the passing wake directly onto the flat-plat at $Re_\theta = 80$, see Wu *et al.* (1999). The skin-friction coefficient C_f follows the Blasius profile for a significant part of the domain for the constrained wake setup, which cannot be said of the unconstrained design, see figure 2. We also consider the minimum C_f station as the statistically averaged location of the breakdown events, which, in turn, divides the transitional region into the early and late transitional stages. The averaged breakdown locations are at $Re_\theta = 250$ and 260 for the unconstrained and constrained designs respectively. The comparison of the skin-friction coefficients achieved in the fully turbulent region, compare well

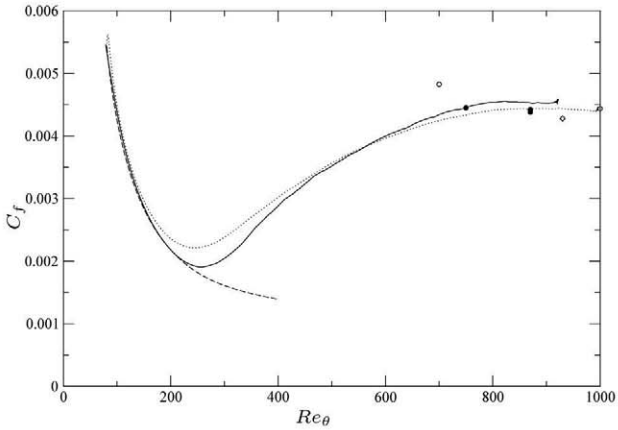

Figure 2: Mean skin-friction coefficient C_f as a function of Re_θ. Solid line: boundary layer with constrained passing wakes; dotted line: boundary layer with unconstrained passing wakes; dashed line: Blasius solution; solid circle: Murlis *et al.* (1982); open circle: Purtell *et al.* (1981); diamond: Adrian *et al.* (2000).

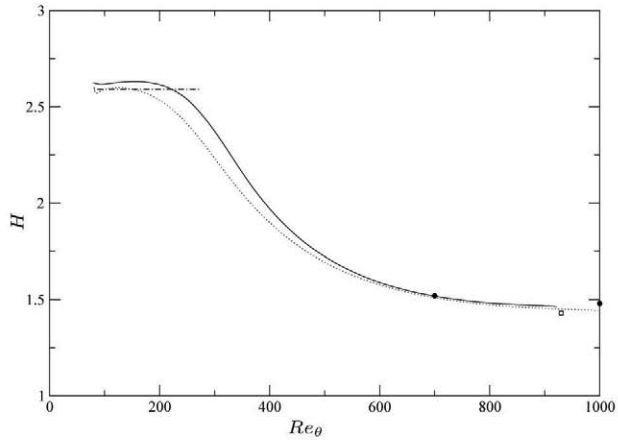

Figure 3: Shape factor $H = \delta^*/\theta$ as a function of Re_θ. Solid line: boundary layer with constrained passing wakes; dotted line: boundary layer with unconstrained passing wakes; solid circle: Murlis *et al.* (1982); box: Adrian *et al.* (2000); chain-dotted line: Blasius solution.

with available experimental data from Murlis *et al.* (1982), Purtell *et al.* (1981) and Adrian (2000).

The shape factor $H = \delta^*/\theta$ as shown in figure 3 is an excellent indicator of the boundary layer transitional state. It is seen that H in the boundary layer with unconstrained inlet wakes deviates from the Blasius value right from the inlet, suggesting that the boundary layer is under finite rather than infinitesimal perturbations. In comparison, H in the boundary layer with constrained wakes follow the Blasius profile until $Re_\theta = 170$. After the completion of transition, both boundary layer shape factors agree well with existing data for canonical turbulent ZPGFPBL.

When simulating the constrained wake design, we observe that the deviation from the Blasius profile is marginal, the disturbances caused by the wake are sufficiently mild and there are no imposed pressure gradients. Consequently, it is fair to assume that the statistics in the late transitional region should converge to the canonical low-Reynolds number turbulent ZPGFPBL profiles in the near-wall region.

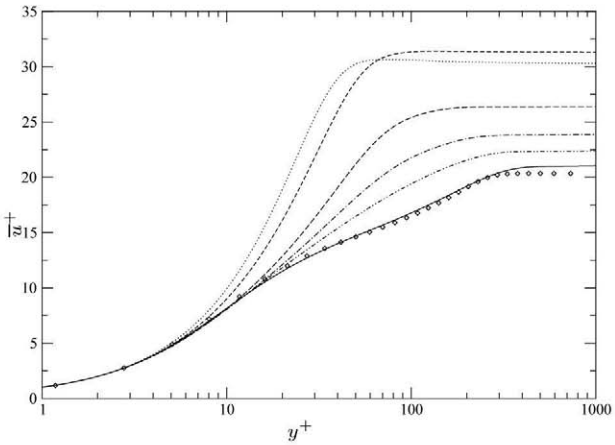

Figure 4: Mean velocity $\overline{u}^+$ as a function of y^+ in the late transitional region of the boundary layer with constrained passing wakes. Dotted line: $Re_\theta = 200$; dashed line: $Re_\theta = 300$; long dashed line: $Re_\theta = 400$; chain-dotted line: $Re_\theta = 500$; chain-dotted-dotted line: $Re_\theta = 600$; solid line: $Re_\theta = 800$; diamond: Spalart (1988) at $Re_\theta = 670$.

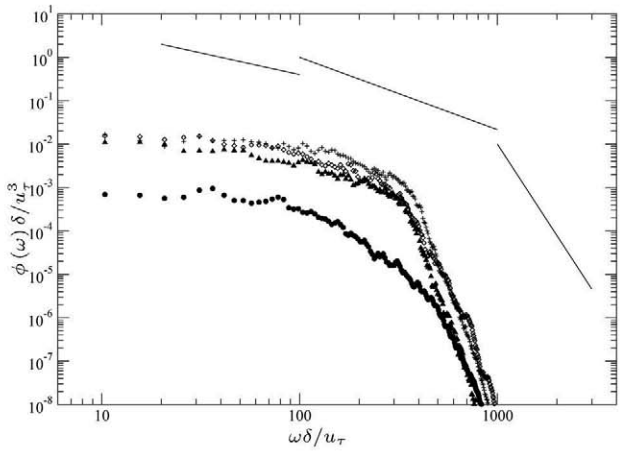

Figure 5: Frequency spectrum of the spanwise velocity fluctuations in the late transitional region of the boundary layer with constrained passing wakes at $Re_\theta = 421$. Circle: $y = 0.027\delta$; diamond: $y = 0.13\delta$; plus: $y = 0.54\delta$; triangle: $y = 1.07\delta$. Solid lines from left to right: -1, $-5/3$ and

The obtained results demonstrate a systematic convergence with increasing downstream position towards the DNS results of the ZPGFPBL by Spalart (1988) as can be seen in figure 4. The comparison between the present results in wall units at the end of the late transitional region, $Re_\theta = 800$, with those of Spalart at $Re_\theta = 670$ are remarkably good. This very good comparison can also be seen in the spanwise and wall normal velocity fluctuations as well as with the Reynolds stress components. This suggests that in the boundary layer with constrained wakes, the inner region after transition can be considered significantly similar to that of a typical ZPGFPBL. The frequency spectrum of the spanwise velocity component for the late transitional region at $Re_\theta = 421$ for the constrained passing wake is presented in figure 5. In the late transitional regions, the high-frequency range shows a fuller profile as compared to the early transitional region in the flow and we note the presence of clearly defined secondary peaks.

STATISTICS IN THE FULLY TURBULENT REGION

Results in the previous section suggest that for the boundary layer with constrained passing wakes, near-wall statistics converge towards those of Spalart (1988) in the late transitional region. Here we present statistics in the fully turbulent region at $Re_\theta = 900$ for the two boundary layers with constrained and unconstrained wakes. The results are compared with low-Reynolds number turbulent ZPGFPBL data. Such an evaluation will help address the issue as to the similarity between the present transitioned turbulent boundary layer and the canonical turbulent ZPGFPBL.

Figure 6 shows the mean velocity $\overline{u}^+$ as function of y^+ from the two boundary layers at $Re_\theta = 900$ together with the data of Murlis *et al.* (1982) and Spalart (1988). The Reynolds stress profiles in figure 7 are compared to four sets of ZPGFPBL data. For the present boundary layers with periodically passing wakes, the values of $-\overline{u'v'}^+$ attain negative values above $y/\delta = 1.2$ while those in the comparative ZPGFPBL remain positive.

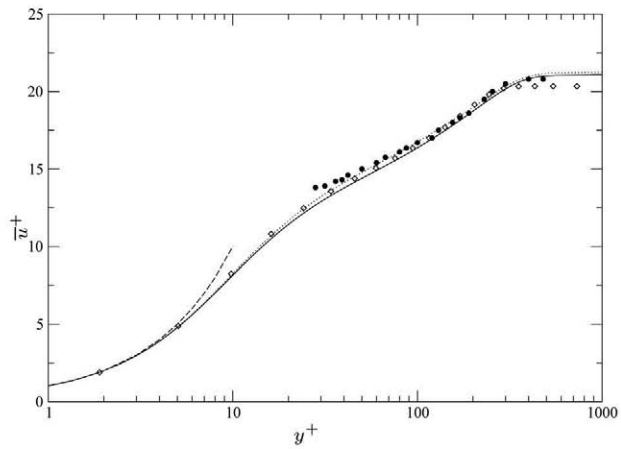

Figure 6: Mean velocity $\overline{u}^+$ as a function of y^+ in the fully turbulent region at $Re_\theta = 900$. Solid line: boundary layer with constrained passing wakes; dotted line: boundary layer with unconstrained passing wakes; dashed line: $\overline{u}^+ = y^+$; circle: Murlis et al. (1982) at $Re_\theta = 791$; diamond: Spalart (1988) at $Re_\theta = 670$.

IDENTIFICATION OF THE BREAKDOWN EVENTS

Having established the quality of the computational results in the last sections, we are ready to address the identified structural issues in flat-plate boundary layer transition with free stream passing wakes through systematic three-dimensional flow visualization. We consider a breakdown event as a modification in any streaky structure in the early transitional region from semi-regular to locally chaotic. Within any particular wake passing period there can be multiple breakdown events. Precise location of the space-time coordinates of the breakdown events is crucial for the determination of breakdown mechanism because processes that occur after breakdown will not be helpful in determining the mechanism that has caused that particular breakdown. We are of the opinion that identification of breakdown events must include the documentation of the relevant development

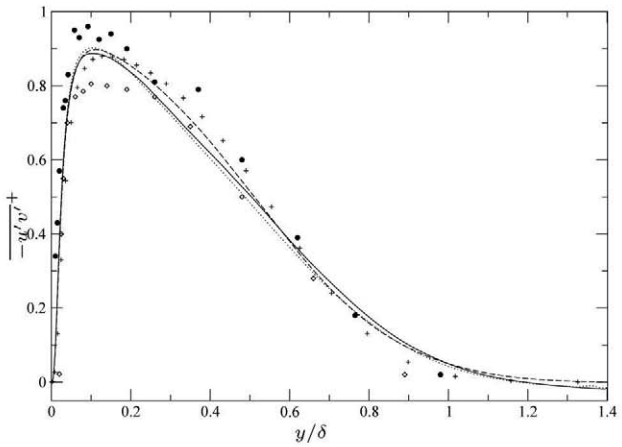

Figure 7: Reynolds shear stresses as a function of y/δ at $Re_\theta = 900$. Solid line: boundary layer with constrained passing wakes; dotted line: boundary layer with unconstrained passing wakes; dashed line: ZPGFPBL of Wu & Moin (2009); circle: Honkan & Andreopoulos (1997) at $Re_\theta = 2790$; diamond: DeGraaff & Eaton (2000) at $Re_\theta = 1430$; plus: Spalart (1988) at $Re_\theta = 670$.

prior to the occurrence of the chaotic scales in the streaks. Presentation of a small turbulent spot does not in itself identify a breakdown event.

For the purpose of this study, we arbitrarily selected the passing period of $t/\mathcal{T} = 39$ without any screening for the constrained design. The visualization is eased by using iso-surface plots of the streamwise velocity u/U_∞, in which a bulge represents a region of negative u'. It can be seen from figure 8, that the streaks are wedge shaped with the strong and narrow end at the trailing edge of the passing wake. The nascent streaks are relatively short and have a total length of approximately 10 local boundary layer thicknesses and as time evolves the streaks lengthen to approximately 20 local boundary layer thicknesses. The figure 8 clearly demonstrated the process of transition for an iso-surface of u/U_∞. The signature of the negative streaky structures near the wall as indicated by bulges near the wall are merely faint foot-prints of the upper layer streaks.

In the unconstrained setup shown in figure 9, the flow is investigated at the randomly chosen period of $t/\mathcal{T} = 30$. There is a qualitative resemblance to the constrained flow setup with regards to the structure of the streaks, but it should be noted that the maximal strength of the streak is found at the upper boundary edge rather than in deep inside the boundary layer as was the case for the constrained wake design.

TRIGGERING MECHANISM FOR BREAKDOWN

Having isolated the breakdown events in the previous section, we now search for processes that occur prior to those events. The first signs of the breakdown can be seen in the form of downstream inclined wrinkle-like wave packets on the flank of the streak, see middle figure 8 for constrained wake and top figure 9 for the unconstrained wake. These three-dimensional structures may be interpreted as small-scale Kelvin-Helmholtz type oscillation along the streamwise direction. As the flow evolves in time, the main body of the streak twists lightly, like a strand. This resembles larger wavelength Kelvin-Helmholtz oscillations over the streamwise-transverse planes of the streak. The breakdown

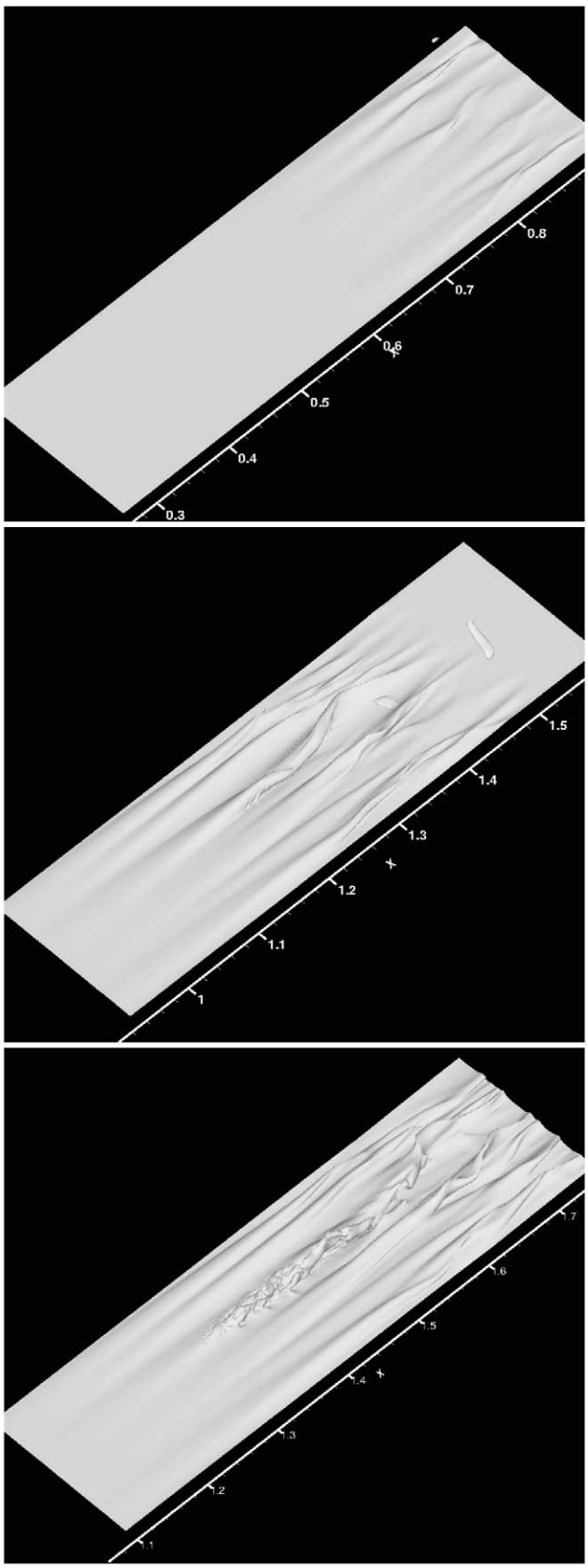

Figure 8: Iso-surface of u in the boundary layer with constrained passing wake at $0.85U_\infty$ at time top : $t = 39.2\mathcal{T}$. Middle: $t = 39.45\mathcal{T}$. Bottom: $t = 39.65\mathcal{T}$. The wrinkles are clearly visible on the flank of the centerline streak.

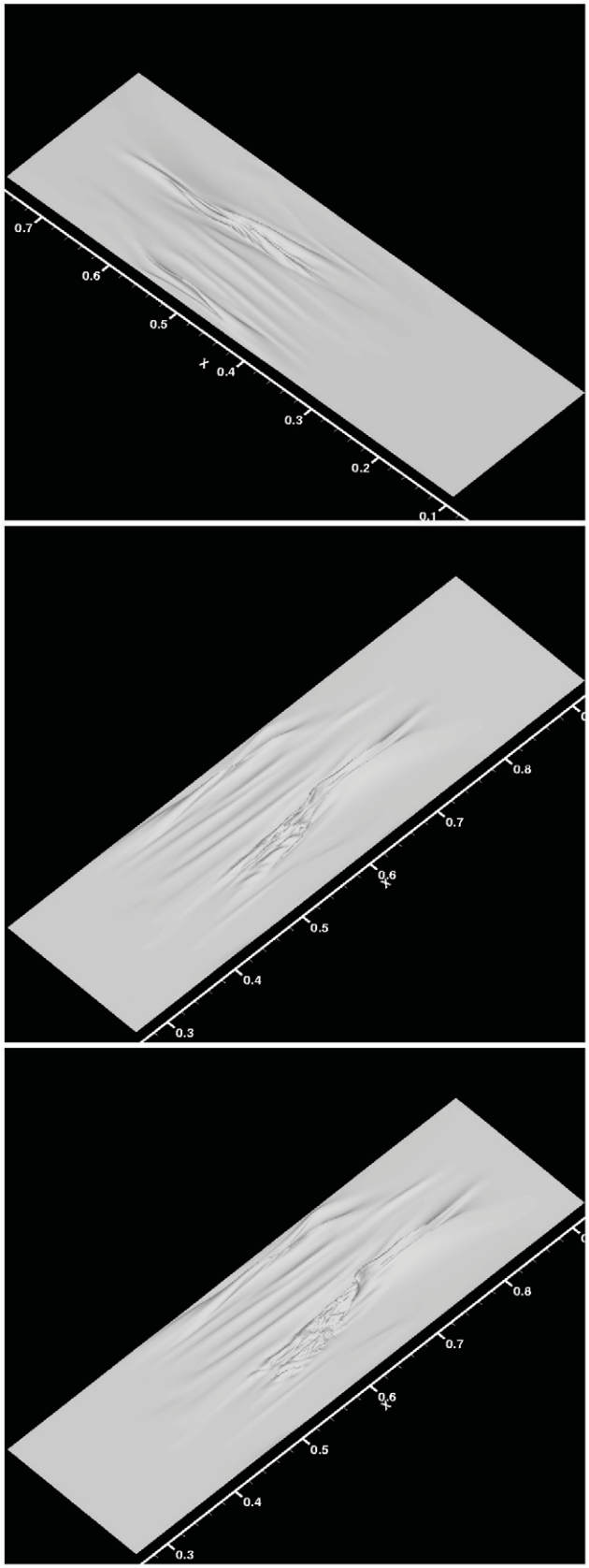

Figure 9: Iso-surfaces of u in the boundary layer with unconstrained passing wakes at $0.7U_\infty$. Top: $t = 30.05\mathcal{T}$. Middle: $t = 30.10\mathcal{T}$. Bottom: $t = 30.15\mathcal{T}$. The view angle was modified in the top figure in order to clearly illustrate the process at hand.

occurs thereafter. The analysis of the iso-surface of different velocities demonstrates that the near-wall portion of the streak remains regular while the outer-layer portion is modified by the small and large-scale Kelvin-Helmholtz oscillations. Both the constrained and unconstrained wakes show a qualitatively similar breakdown mechanism which is summarized in figure 1.

ARROWHEAD DIRECTION OF TURBULENT SPOTS

Wu *et al.* proposed that the direction of matured turbulent spots depend on the relative wall-normal location of the breakdown event in the boundary layer. If breakdown is initiated from the boundary-layer edge, the resulting spot arrow head will point towards the upstream direction. Their reasoning is quite logical and analogous to the explanation given to the phenomenon of Mach cones in compressible flow. More recent authors have paid little attention to the issue except for Antony *et al.* (2005), who reported that they found no evidence to support the idea of Wu *et al.* (1999). Here we present visualizations to show that the reasoning of Wu *et al.* is indeed sound.

For the boundary layer with constrained passing wakes, after breakdown of the negative streak at $t/\mathcal{T} = 39.65$ a turbulent spot develops from the shape of a narrow stripe into a wedged shape with a distinct arrowhead pointing in the upstream direction. In the unconstrained case, the turbulent spot develops from a simultaneous breakdown of two neighboring streaks near the center plane. This causes the loss of a clear arrowhead in the merged turbulent patch. It should be recalled that the flow visualizations presented in this paper were randomly picked without pre-screening or post-screening.

CONCLUSION

The problem of flat-plate boundary layer under the disturbance of a free-stream periodic wake disturbances, is a well-defined, idealized laboratory flow with sufficient scientific generality and good engineering relevance. The quality of our numerical simulation can be seen through the comparison with classical experimental data of the ZPGFPBL. This comparison lends credibility to our flow visualization study of the breakdown mechanism. The transition to turbulence was initiated by small-scale wrinkle-like Kelvin-Helmholtz wave packets superimposed on the flanks of some selected streaky structures, near the boundary layer outer edge. Shortly thereafter, the affected negative streaks start to get twisted near the location of the wrinkles possibly due to strong large wavelength Kelvin-Helmholtz oscillations. This process develops to include a significant portion of the main body of the streaks, which directly results in a breakdown.

REFERENCES

Adrian, R. J. , Meinhart, C.D. & Tomkins, C.D., 2000, "Vortex organization in the outer region of the turbulent boundary layer", *J. Fluid Mech.*, 422, 1–54.

Anthony, R. J., Jones, T. V. & LaGraff, J. E., 2005, "High frequency surface heat flux imaging of bypass transition", *J. turbomachinery*, 127, 241–250.

Brandt, L., Schlatter, P. & Henningson, D. S.," Transition in boundary layers subject to free-stream turbulence", *J. Fluid Mech.*, 517, 167–198.

DeGraaf, D.B. & Eaton, J. K., 2000, "Reynolds-number scaling of the flat-plate turbulent boundary layer", *J. Fluid*

Mech., 422, 319–346.

Hodson, H.P. & Howell, R.J., 2005, "Bladerow interactions, transition and high-lift aerofoils in low-pressure turbines", *Annu. Rev. Fluid Mech.*, 37, 71–98.

Honkan, A. & Andreopoulos, Y., 1997, "Vorticity, strain-rate and dissipation characteristics in the near wall region of turbulent boundary layers", *J. Fluid Mech.*, 350,29–96.

Jacobs, R.G. & Durbin, P.A., 2001, "Simulation of bypass transition", *J. Fluid Mech.*, 428, 185–212.

Liu, X. & Rodi, W., 1991, "Experiments on transitional boundary layers with wake-induced unsteadiness", *J. Fluid Mech.*, 231, 229–256.

Murlis, J., Tsai, H.M. & Bradshaw, P., 1982, "The structure of turbulent boundary layers at low Reynolds numbers", *J. Fluid Mech.*, 122, 13–56.

Purtell, L. P., Klebanoff, P.S. & Buckley, F. T., 1981, "Turbulent boundary layer at low Reynolds number", *Phys. Fluids*, 24, 802–811.

Spalart, P. R., 1988, "Direct simulation of a turbulent boundary layer up to $Re_\theta = 1410$", *J. Fluid Mech.*, 187, 61–98.

Stieger, R. D., 2002, *The effect if wakes on separating boundary layers in low pressure turbines*, Ph.D Thesis, University of Cambridge, UK.

Stieger, R. D. & Hodson, H.P.,2004, "The transition mechanism of highly loaded low-pressure turbine blades" *ASME J. Turbomachinery*,126, 536–543.

Wu, X. , Jacobs, R. , Hunt, J.C.R. & Durbin, P.A. (1999), "Simulation of boundary layer transition induced by periodically passing wakes", *J. Fluid Mech.*, 398, 109–153.

Wu, X. & Moin, P., 2009, Direct numerical simulation statistics of a nominally zero pressure gradient flat-plate boundary-layer, accepted for publication in *J. Fluid Mech.*